Cold Outflow from the Faroe Bank Channel

P. M. SAUNDERS

Institute of Oceanographic Sciences, Deacon Laboratory, Wormley, Godalming, Surrey, U.K.

(Manuscript received 27 February 1989, in final form 20 July 1989)

ABSTRACT

The exchange of water between the Norwegian Sea and the North Atlantic around the Faroe Islands was investigated in 1987 and 1988 combining CTD data with shipborne Acoustic Doppler Current Profiler (ADCP) measurements. Tests were devised to assess the accuracy of the ADCP measurements and the results are described; it is found that estimating a reference velocity for geostrophic measurements is limited by the presence of tides of order 10 cm s^{-1}. In the outflow of cold water from the Faroe Bank Channel, which reaches speeds of nearly 1 m s^{-1}, the error is acceptably small but strong time dependent components are revealed. The discharge of cold water is traced 75 km beyond the sill of this channel and changes in potential temperature, salinity and potential vorticity on an isopycnal surface are attributed to intense mixing. An effective diffusivity near 100 $cm^2 s^{-1}$ is derived and K–H instability demonstrated as a plausible source of the turbulent energy. Six current meter moorings were deployed from spring 1987 to spring 1988 near the sill of the Faroe Bank Channel but only two were recovered. Striking time dependence is seen at periods between 3 and 6 days mostly confined to the warm upper layer, but the origin and nature of these motions is not found. Seasonal signals are sought and none found in the cold outflow. This surprising result encourages the author to combine long-term current measurements with CTD and ADCP data and determine the flux of water colder than 3°C from the Faroe Bank Channel as $(1.9 \pm 0.4) \times 10^6$ $m^3 s^{-1}$.

1. Introduction

NANSEN (North Atlantic–Norwegian Sea Exchange) is a programme sponsored by the ICES nations to investigate the fluxes of heat and salt and other trace gases across the Greenland–Iceland–Scotland ridge. As well as assessing their seasonal and interannual variation, it is hoped that such measurements can be made with sufficient precision to be of use in climate modeling and as boundary conditions to the North Atlantic ocean circulation models envisaged in WOCE.

Within this framework, measurements of the overflows of Norwegian Sea water into the North Atlantic were undertaken (for historical reviews of previous programmes see Meincke 1983 and Swift 1984). Between Iceland and Scotland the overflows emerge sporadically through the deepest channels in the ridge between Iceland and the Faroe Islands but steadily and persistently only from the Faroe Bank Channel whose sill lies southwest of the Faroes (see Fig. 1). Recent measurements have been reported from this channel by Borenäs and Lundberg (1988) who also summarized previous measurements there: all, including theirs, are of short duration.

Interest in long term observations was stimulated by data gathered along the edge of the Hebridean Shelf near 61°N, 2°W (Gould et al. 1985). These authors discovered a strong seasonal modulation of the inflow of warm North Atlantic water into the Norwegian Sea, doubling in late winter compared with late summer. It was supposed a similar signal might be seen in the contrary current, the deep overflow if only to prevent unreasonable mass accumulations (deficits) taking place.

In setting current meter moorings in the Faroe Bank Channel a spacing of about 5 km was selected in order to define the flux of cold water with sufficient accuracy: previous experience from a gap of comparable width (Saunders 1987) had shown how small scale the flow variation could be. The threat from commercial fishing was recognized but local advice suggested that provided moorings were confined in the vertical the risk was small; a depth of 300 m was set as their limit. A sketch of the array consisting of six moorings instrumented with 17 current meters and 3 thermistor chains is shown in Fig. 2; this was deployed in the Spring of 1987 from the RRS *Challenger*, Cruise 15/87.

In addition to the moored current measurements a series of CTD sections were undertaken within the Faroe Bank Channel, on the Wyville–Thomson Ridge, within the Faroe–Shetland channel as well as north and west of the Faroe Islands (see Fig. 1). The sections were unique, because for the first time an acoustic doppler current profiler (ADCP) was available to us and the measurements could be combined with the hydrography to yield direct observations of fluxes

Corresponding author address: Dr. Peter M. Saunders, Institute of Oceanographic Sciences, Deacon Laboratory, Brook Road, Wormley Godalming, Surrey GU5 8UB, United Kingdom.

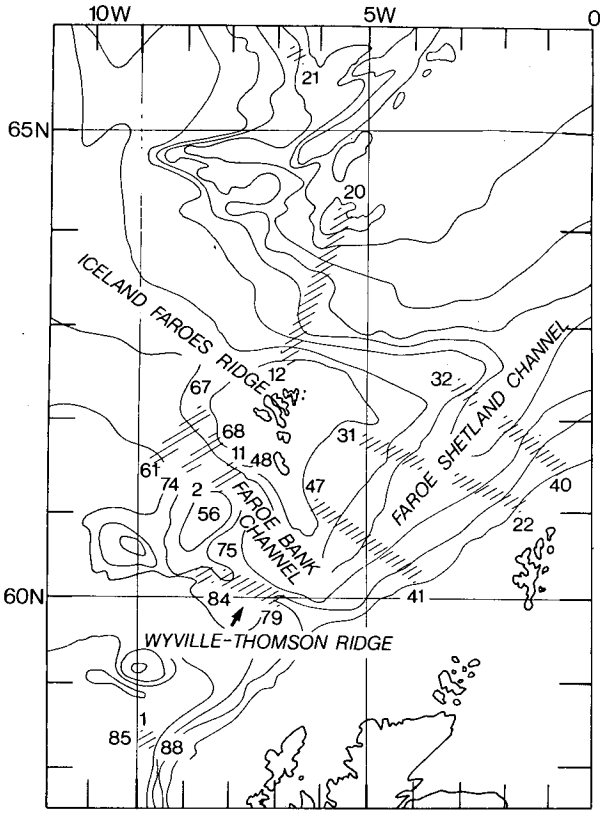

FIG. 1. The area covered in this article. CTD/ADCP sections and key geographical locations are indicated. The moorings (Fig. 2) are located at the CTD section comprising stations 2–11, 48–56 and is also the location of stations 11734–41.

without appeal to the concept of "the level of no motion." In addition the CTD stations were made to establish a modern water mass census for the region, to quantify changes taking place within the region and to aid in an understanding of the dynamics of the cold water outflow.

Although the current measurements were the focus of this investigation, heavy mooring losses were encountered; consequently precedence is given to the hydrography and shipborne acoustic doppler observations.

2. Shipborne measurements

Two visits were made to the region of the Faroe Islands, the first on RRS *Challenger* (Cruise 15) in the spring of 1987 and the second on RRS *Discovery* (Cruise 174) in the spring of 1988. Nearly 90 CTD stations were made on the *Challenger* cruise, during which the current meter moorings were deployed, and 10 on the *Discovery* cruise during which recoveries were planned. Most of the analysis therefore concentrates on the *Challenger* data which predominates.

CTD stations were made with a NBIS instrument (Mark III), 1 m path transmissometer from Sea Tech, Inc., and a General Oceanics multisampler in a side-by-side configuration. A general review of IOS procedures is found in Saunders (1985). A list of station positions as well as lists and graphs of the data have been prepared and, for the *Challenger* cruise, published (Saunders and Gould 1988). Because of a defective sensor, oxygen measurements were not made and of the nutrients only silicate was measured; see the data report for further details.

An RDI Systems 150 kHz acoustic doppler current profiler was installed on the Challenger and operated under the control of company supplied software: the instrument worked well. Data was transferred via a real-time link from the deck unit, an IBM PC to a PDP 11/34. Within two hours of logging, ADCP data was available for analysis off-line.

a. Acoustic Doppler current profile data

Acoustic Doppler profile data was gathered at a 3 minute sampling interval into 75 depth bins with a separation of 8 m, the shallowest centered on 10 m and the deepest on 602 m. Bottom tracking was accomplished to a depth of 525 m on the *Challenger* Cruise and improved to nearly 700 m on the subsequent *Discovery* cruise. In the water tracking mode depths of 400 m were rarely exceeded on the *Challenger* and often were only one-half of this on the *Discovery*.

A method of checking the performance of the instrument has recently been described by Pollard and Read (1989) following principally on the work of Kosro (1985). Such procedures require the use of precise more-or-less continuous navigation systems (GPS or

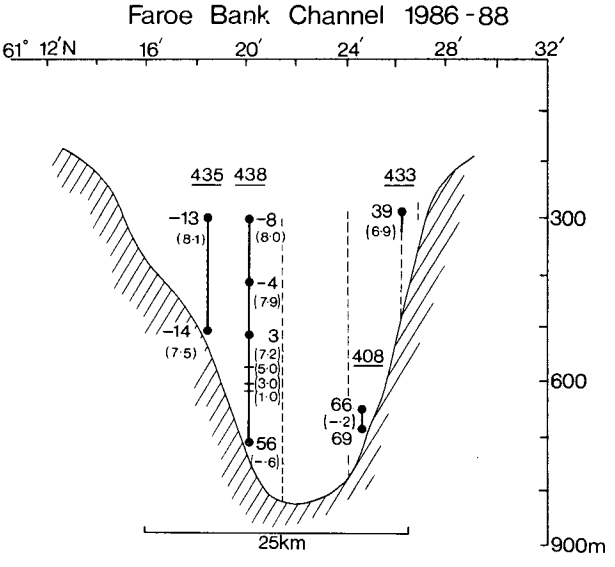

FIG. 2. Moorings in the Faroe Bank Channel: mooring numbers are underlined. Record mean values of NW component cm s^{-1} and temperature °C alongside instruments: temperature in parenthesis. Chain lines indicate moorings not recovered.

loran) which were not available on the *Challenger* cruise. Accordingly alternative checks were devised and these are described in detail in the Appendix to this paper. Suffice it to say that our tests revealed that when underway in the bottom tracking mode the ADCP speed needed no correction but had an instrument/gyro misalignment of approximately 0.5° to port. In the water tracking mode the misalignment angle was the same but the speed read low, requiring a correction of 1.5%. These corrections have been made.

A limited number of comparisons were made by averaging the ADCP profiles between the CTD stations of a section and resolving the average components normal to the section. These profiles were compared with geostrophic shear profiles and the results for two sections shown in Fig. 3. Geostrophic profiles have been superimposed in such a way as to maximize agreement; in the Faroe Bank Channel (upper two panels) the agreement is excellent. In the Faroe–Shetland Channel (lower two panels) some marked discrepancies are revealed. The latter result should come as no surprise: the ADCP measures any ageostrophic component of the flow and in the upper 400 m of the water column both inertial oscillations and internal tides have amplitudes of 5 cm s^{-1} in this area (author's own data).

The ADCP data also contains ageostrophic barotropic tidal currents. From the numerical modeling of Flather (1986) tidal currents have been determined on a grid (0.5° long × 0.3° lat) for a number of constituents; the semidiurnal lunar tide M_2 dominates. In the channels around the Faroes the tidal amplitude is found close to 10 cm s^{-1} and in shallower water it is considerably stronger, viz. 30 cm s^{-1} at the 100 m isobath. In combining geostrophic estimates with ADCP data a reference level of 300 m has been selected, identifying the geostrophic current there with the ADCP values averaged between stations. Resulting errors in the geostrophic flow must be of the order of 10 cm s^{-1} given the tidal and inertial signals. On a CTD section of long duration, of many tidal and inertial periods, such ageostrophic signals might be expected to average to zero. On the short CTD sections reported here, of duration between ½ and 1 day, section average velocities might have errors of only 2 cm s^{-1}. But where inflows and outflows are concentrated, often crossed in only 3 hours, the large errors would persist. Thus, although Pollard and Read assert that a well-calibrated ADCP (such as existed for the *Challenger* cruise) may have errors of 5 cm s^{-1} it is argued here that, when combining ADCP and CTD data an even larger error, here 10 cm s^{-1}, can result from the presence of ageostrophic flow components in the ADCP data.

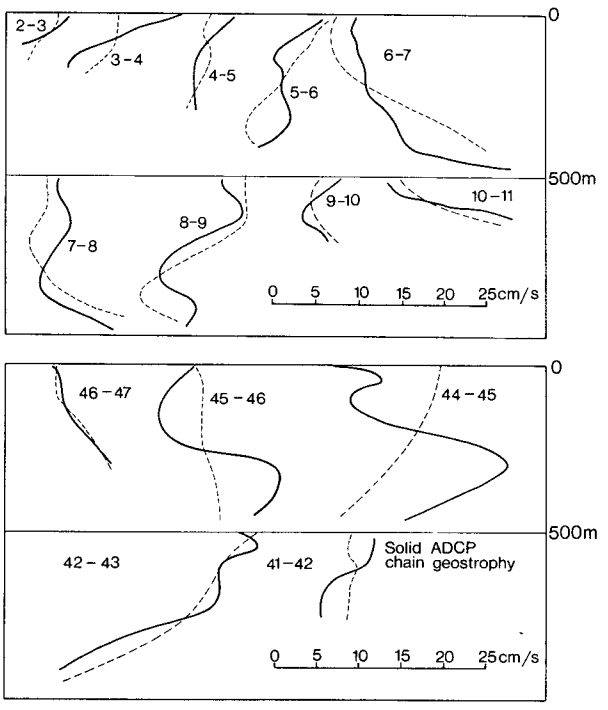

FIG. 3. Geostrophic current profiles for pairs of CTD (station numbers indicated) superimposed on spatially averaged ADCP estimates derived from underway data. Upper panels from Faroe Bank Channel, lower from Faroe Shetland Channel.

b. Current and temperature sections

1) WARM WATER EXCHANGE

The warm water inflow from the North Atlantic to the Norwegian Sea along the Hebridean Shelf was measured by Gould et al. (1985), apparently settling the contradictory estimates of Worthington and Tait (Worthington 1970) as to its magnitude in favor of the former. The southern section in the Faroe Shetland Channel (Fig. 1), comprising stations 41–47, reveals this warm current with a core speed of 40 cm s^{-1} (Fig. 4). On this section stations are 20 km apart. From the combined CTD and ADCP measurements the transport of warm water (>7°C) is determined as $(5.3 \pm 1.5) \times 10^6$ m^3 s^{-1}, consistent with the springtime estimates by Gould et al. On the two sections farther north (not shown here) core speeds had fallen and the uncertainties became comparable to the estimate.

North of the Faroe Islands the CTD section comprising stations 12–20 reveals the presence of warm modified North Atlantic water (Fig. 5). This water travels along the south side of the Iceland–Faroes Front, revealed by the SeaSoar survey carried out on the *Challenger* cruise (Gould et al. 1987), and passes north of the Faroes. The eastward transport of water warmer than 5°C is estimated to be only $(0.5 \pm 1.0) \times 10^6$ m^3 s^{-1}. A contemporary satellite IR image, printed in Gould et al. reveals a convoluted thermal structure at the location of the CTD section; thus the value obtained is almost certainly unrepresentative. Certainly it is smaller than the value of 3×10^6 m^3 s^{-1} derived at the same location for a ten-day period in the summer of 1986 (Hansen et al. 1986).

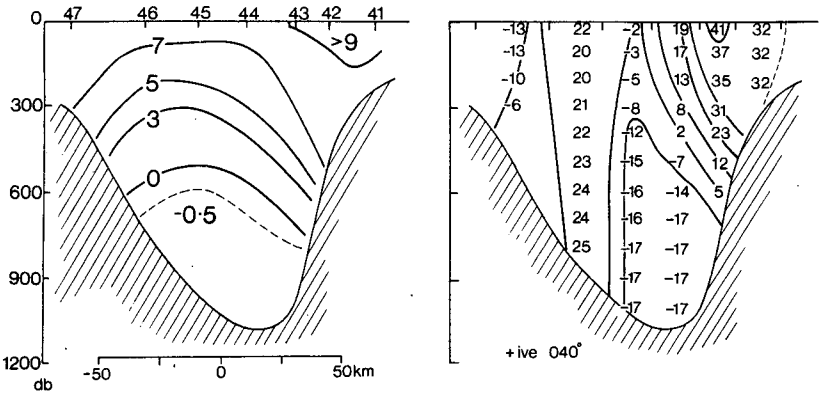

FIG. 4. On left, isotherms from CTD stations (numbered at top); on right, normal component of current (cm s^{-1}) derived by combining geostrophic estimates with ADCP values at 300 m. The direction of +ive components is shown. Faroe Shetland Channel-south end, 25 May 1987.

The results for the warm water exchange found on *Challenger* Cruise 15/87 are quite at variance with a recent analysis of CTD data in the same region by van Aken (1988) who utilized 173 stations and mass conservation principles. Note that van Aken's measurements were made in the summer of 1983 when Gould et al. began their measurements. Van Aken concluded that the warm water inflow to the Norwegian Sea occurred principally north of the Faroes. Unfortunately he had no current measurements as further constraints on his data; if he had employed them radically different results might have emerged.

2) COLD WATER EXCHANGE

The majority of the CTD sections were designed to observe the cold outflow from the Norwegian Sea. In Fig. 4 cold water is seen recirculating within the Faroe–Shetland Channel: the net transport of water colder than 3°C is quite uncertain (1.7 ± 2.5) $\times 10^6$ m^3 s^{-1}. Similarly uncertain values have been derived from the two other sections occupied in the Faroe–Shetland Channel and illustrate the weakness of the method used when maximum currents are only 10–20 cm s^{-1}.

Alongside the moored current meters (see Fig. 1) near the channel sill, CTD sections comprising stations 2–11 (Fig. 6), stations 48–56 (Fig. 7) and *Discovery* stations 11734–41 (Fig. 8) have been worked and the geostrophic estimates combined with ADCP data. Features common to all three sections are: 1) the northwest outflow of cold water is relatively uniform and ranges between 35 and 70 cm s^{-1} and 2) on the north side of the channel the warm water flow is also northwest (circa 30 cm s^{-1}) but on the south side the warm water flow is southeast. It will be noted that these warm water flows both correspond to anticyclonic circulation around topography, viz. the Faroe Plateau to the north and the Faroe Bank to the south. The strength of the cold outflow is quite different on the three occasions; mass fluxes will be described in a later paragraph.

A section comprising stations 68–74 was occupied 45 km beyond the sill of the Faroe Bank Channel (see Fig. 1): the cold outflow is intense on the northern side

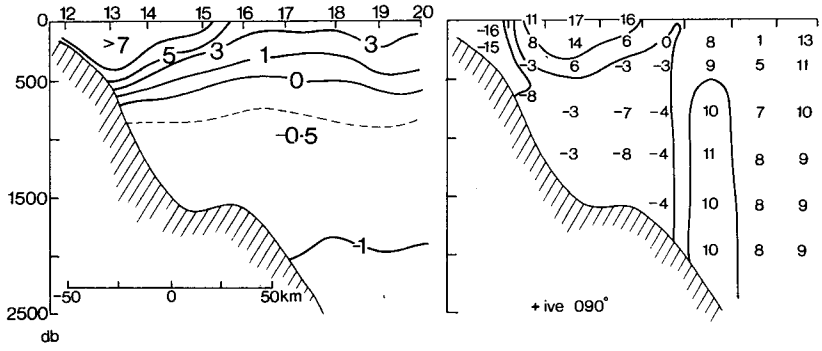

FIG. 5. As in Fig. 4. North of the Faroe Islands, 13/14 May 1987.

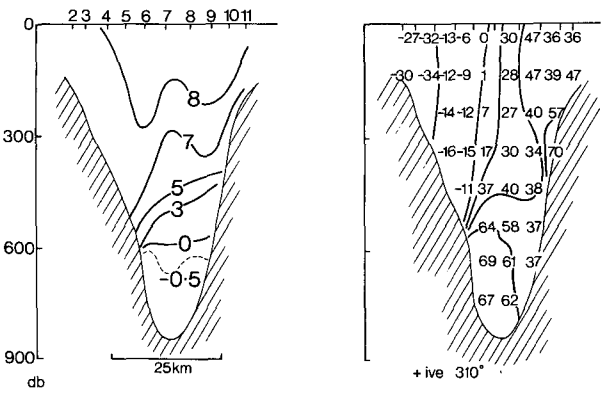

FIG. 6. As in Fig. 4. Faroe Bank Channel, 12 May 1987.

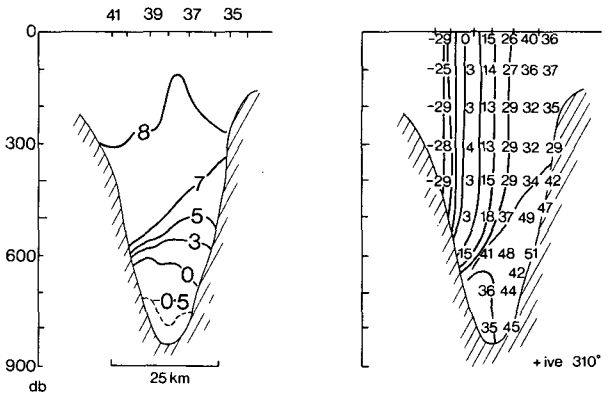

FIG. 8. As in Fig. 4. Faroe Bank Channel, 22/23 May 1988.

but weak on the southern (Fig. 9). The strong outflow of warm water above the cold outflow is again evident. A further 30 km to the northwest a section comprising stations 61–67 was occupied; the overflow water (Fig. 10) is seen as a cold lens perched on the slope. Deep currents are still strong but surface currents are now weak. The coldest water is noticeably warmer than that at the sill in the Faroe Bank Channel. This section was reoccupied in the spring of 1988 (not shown here) and although the isotherm locations and currents are quite similar, no water as cold as 0° was found. A relative dearth of cold water is seen in the Faroe Bank Channel (Fig. 8) at the same time.

The last current/temperature sections to be presented are from the Wyville–Thomson Ridge where a notch allows cold overflow water to escape from the flanks of the Faroese channels. These (Figs. 11, 12) were made in the spring of 1987 and 1988 and illustrate quite different modes of overflow. Stations 75–79 supplemented by XBTs reveal a small region of overflow embedded within strong flows of warm water; above and west of the notch the flow is southward and east of it is northward. In 1988 data was obtained from XBTs only; using the T–S relation found in the previous spring geostrophic currents were computed and combined with 200 m ADCP measurements (Fig. 12). The outflow is displaced to the west but paradoxically the flow of warm water is northward there and southward to the east of the notch; that is the reverse of 1987 and considerably weaker.

3) THE LEVEL OF NO MOTION

In the absence of measurements of current, the thermal wind equation leaves undefined an additive velocity component. Choosing a pressure level (or density surface) of zero motion, often as deep as the observations extend, is a hallowed practice. And more sophisticated techniques, such as the inverse method, start out in the same way. In the relatively shallow channels around the Faroe Islands this concept does not appear to be confirmed by the ADCP measurements. On most of the sections the zero velocity isotach appears to be nearly vertical, cutting across any surfaces or levels: barotropic components of the flow are large and exceed 10 cm s^{-1}, the assumed upper bound on the tidal component. As examples note the warm inflows on the West Shetland Shelf (Fig. 4), on the Wyville–Thomson Ridge (Fig. 11), and the anticyclonic flow around the Faroe Island Plateau (Fig. 6 at seq.) which augments

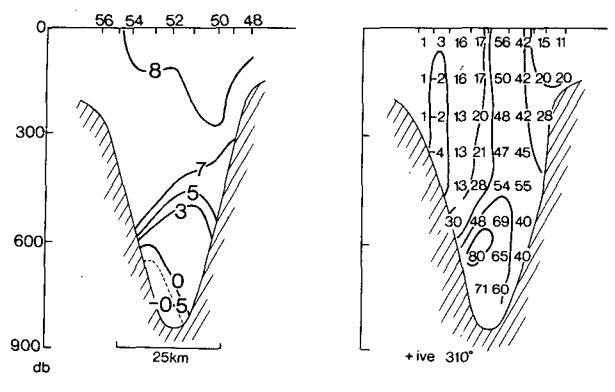

FIG. 7. As in Fig. 4. Faroe Bank Channel repeat, 26/27 May 1987.

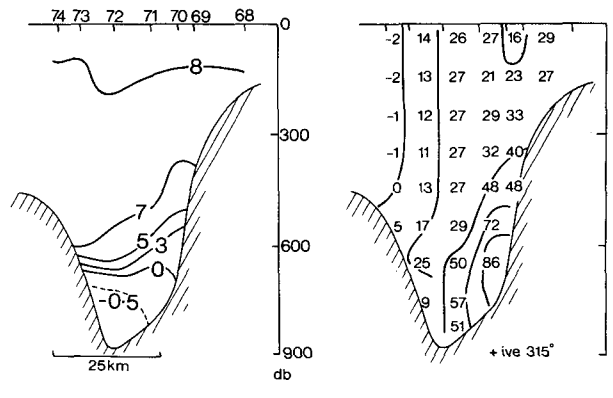

FIG. 9. As in Fig. 4. Exit of Faroe Bank Channel, 30 May 1987.

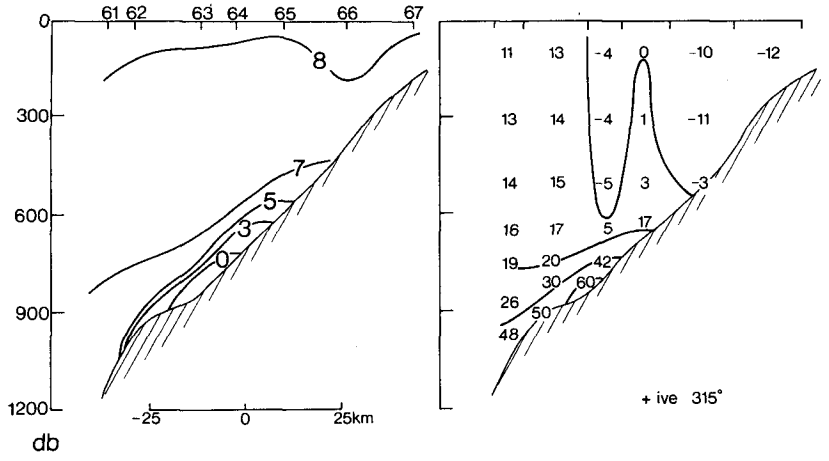

FIG. 10. As in Fig. 4. Iceland–Faroe Ridge, 29/30 May 1987.

the deep outflow in the Faroe Bank Channel. When the moored current measurements are discussed it will be seen that those barotropic components also have large mean values.

A second and perhaps less surprising feature of the current sections is to be found in their time dependence. In these regions of shallow topography repeated hydrographic sections separated either by days or a year have shown only broad areas of agreement: details always differ. Thus we expect and find differences in the flow field. These differences (see Figs. 6, 7) illustrate the power of the ADCP technique but also indicate the impossibility of estimating "average" flow conditions from anything other than many experimental realisations.

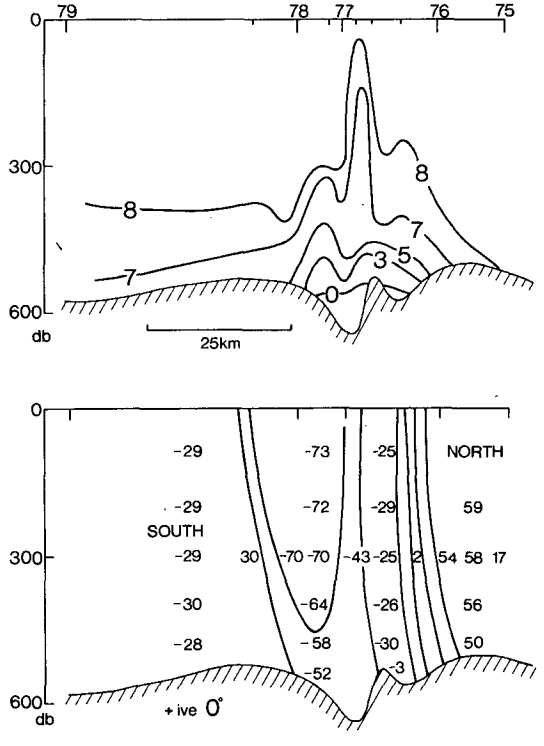

FIG. 11. As in Fig. 4. Wyville–Thomson Ridge, 1 June 1987.

4) COLD WATER FLUXES

From the current/temperature sections the transport of mass or flux of cold water can be estimated. The data for the *Challenger* Cruise 15 (1987) is displayed in Fig. 13. Calculations have been made of the flux of water colder than 3°C (following Dooley and Meincke 1981) and the flux of water colder than 0°C: the units are $10^6\ m^3\ s^{-1}$ (Sv) or $10^9\ kg\ s^{-1}$. In the main channels values of the former quantity vary between 1 and 2.4 and of the latter between 0.5 and 1.7. Former values are quite similar to those recently reported by Borenäs and Lundberg (1988) who also reviewed earlier estimates. A flux of cold water has also been estimated across the Wyville–Thomson Ridge as 0.35 Sv for water colder than 3°C, agreeing reasonably with an estimate of Ellett and Edwards (1978). In 1988 an additional section was occupied using XBTs and a corresponding value of 0.3 Sv was determined: these illustrate that a small but perhaps not negligible amount of overflow water escapes into the north end of the Rockall Trough, rather than into the Iceland Basin.

Borenäs and Lundberg argued that their measured flux in the Faroe Bank Channel agreed with their predictions for rotating stratified flow in a channel subject to hydraulic control at the sill. Their most detailed results are presented for a channel of parabolic cross section with two fluid layers of which only the lower one is active. Values of transport (colder than 3°C) were calculated across the sill of maximum depth 850 m as between 1.5 and 2.5 Sv for upstream "inlet" depths of the 3°C isotherm between 500 and 400 m. However, they pointed out that the 3°C isotherm surfaced in the

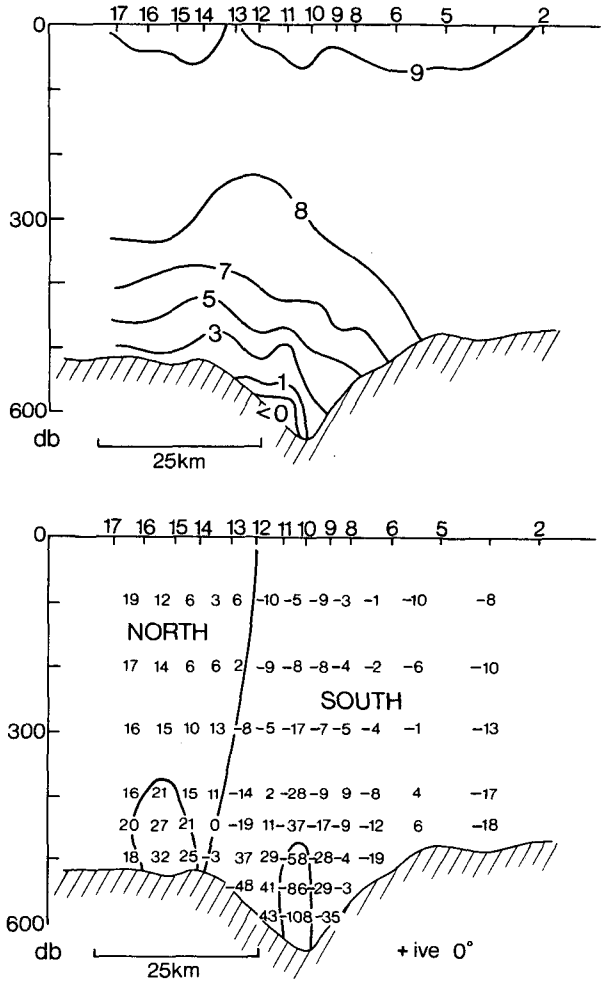

FIG. 12. As in Fig. 4. Wyville–Thomson Ridge, 21 May 1988.

Norwegian Sea and a choice of inlet depth at the surface leads to unrealistically large outflows since the flux depends on the square of the height of the inlet interface reckoned above the sill. The choice that is made is justified, weakly in our view, by arguing that a limiting solution exists with zero velocity on the north side of the channel. For this solution the depth of interface at the inlet equals its minimum depth on the sill section: in their observations a 400–500 m depth was a reasonable choice, but is not such a good choice in the data presented here. According to my calculations their solution predicts an interface that slopes very steeply across the channel, falling from 500 m on the north side to 750 m on the south side where the cold outflow speeds are 150 cm s^{-1}. These details do not agree well with either their observations or ours.

In addition to these difficulties Borenäs and Lundberg admit two weaknesses to their model, an inactive upper layer and inlet potential vorticity for the lower layer set equal to zero. This latter assumption leads to relative vorticity of the deep flow equal to $-f$ everywhere in the channel whereas their estimates from data on the sill section are only $-0.1f$ to $-0.2f$. They have relaxed this condition without appreciably changing the flux of cold water, but modifications to the other conditions of the discharge are not described. We agree with Borenäs and Lundberg that a quantitative theory for the discharge is an important goal: how else, in the near future, may estimates be made of the impact of climatic change on the strength of the overflow and hence on the production of deep water? But in our judgement a considerable gap exists between theory and observation that remains to be bridged.

c. *Water masses and mixing*

Four major water types have been identified in the Iceland Scotland region. The terminology of Dooley and Meincke (1981) is adopted here, closely following early analyses by Hermann (1967). In the following paragraphs three of the four will be encountered: modified North Atlantic water (MNA) a warm near surface layer; Arctic intermediate water also designated NI/AI to take account of an admixture of North Iceland winter water; and Norwegian Sea deep water (NS) found at the bottom of the Faroese channels. Those water types, arranged vertically in the water column, vary somewhat from season to season and the literature cited should be consulted for their characteristics (see also Fig. 15).

The coldest water in the Faroese channels has its origins in the southern Norwegian Sea from a depth near 1000 m (Swift 1984). This level is much shallower than 2000 m where the Norwegian Sea deep water with potential temperature $\theta \leq -1.05$°C is found: so the abbreviation NS should be used with caution.

Much previous research into the hydrography of the

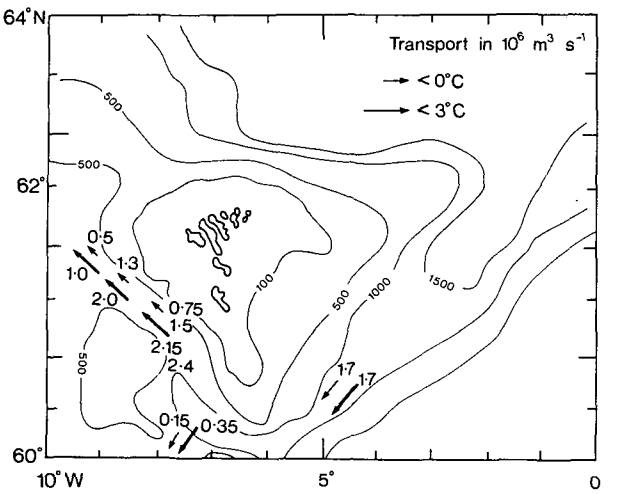

FIG. 13. Transport in 10^6 m^3 s^{-1} derived from CTD/ADCP sections in 1987. Bold arrows for water colder than 3°C, light arrows colder than 0°C.

area between Scotland and Iceland has been given to determining the percentage of the above water types from which a water mass of arbitrary θ–S must be composed. If only three sources are assumed such a specification is unique. A fruitful example of such an analysis is found, for example, in the percentage of NS water present in the cold overflow near the seabed on the lower flanks of the Iceland–Faroes ridge (Swift 1984). Before presenting an example of this technique, property distributions on an isopycnal surface will be considered.

In previous paragraphs attention has been focused on the surface at 3°C, a midthermocline temperature employed to distinguish between "warm" and "cold" layers: this surface is close to the isopycnal $\gamma_0 = 27.9$ kg m^{-3}. ($\gamma_0 = \rho - 1000$ is the potential density excess reckoned for zero pressure). Van Aken (1988) points out that this surface lies centrally in the range of NI/AI water and plotted the salinity on it (his Fig. 3b). In 1983 salinities in the Faroe–Shetland Channel were less than 34.85 and in the Faroe Bank Channel were

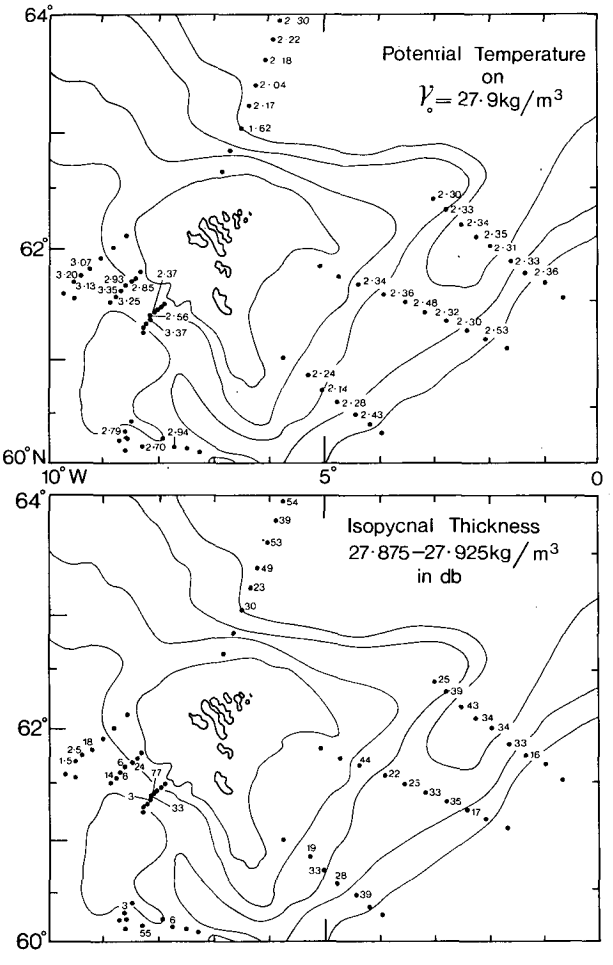

FIG. 14. Properties on the potential density surface $\gamma_0 = 27.9$ kg m^{-3}. Upper, potential temperature, °C; lower, thickness in db of layer indicated.

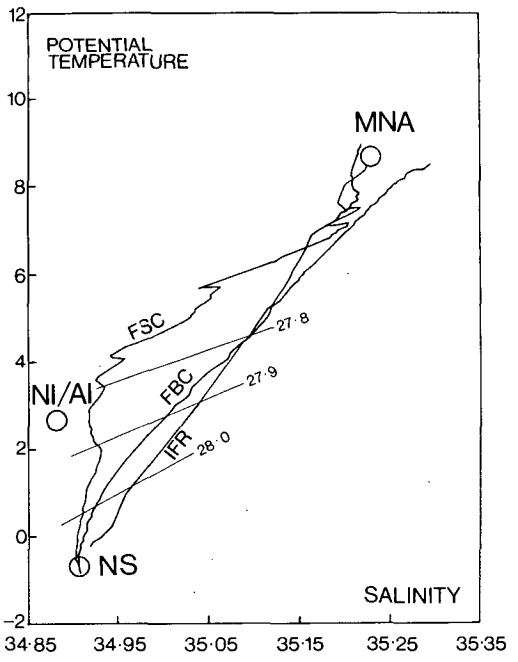

FIG. 15. Potential temperature–salinity plot for selected stations (see text). Water types are indicated MNA, NI/AI, NS along with potential density γ_0.

34.95: *Challenger* data from 1987 shows water considerably more saline, 34.94 and 34.99 respectively, for the same location and therefore containing a smaller percentage of NI/AI water. The 1987 data is displayed in more detail in Fig. 14a, showing the distribution of θ on this surface; its depth is generally 400–600 m. In the Faroe–Shetland Channel θ is approximately 2.3°C whereas it is slightly lower north of the Faroes (2.0° to 2.2°C). In the Faroe Bank Channel values range between 2.35° and 3.35°C and on the Iceland–Faroes ridge all exceed 3°C.

To explain this variation, θ–S plots for selected CTD stations are presented (Fig. 15): stations with the lowest bottom temperatures have been selected from the Faroe–Shetland Channel FSC (station 45), Faroe Bank Channel FBC (8) and the Iceland–Faroe ridge IFR (63). Also shown are the characteristics of three water masses slightly modified from the observations of Müller et al. (1979). According to the ideas of the authors cited earlier, the θ–S for the IFR station can be constructed from a mixture of MNA and NS waters alone. At the FBC site the θ–S is similar but for $\gamma_0 > 27.8$ kg m^{-3} requires between 0% and 20% of NI/AI water added. At the FSC site, for $\gamma_0 < 27.8$ the mixture is almost solely between MNA and NI/AI waters: at deeper levels on this station all three water masses are involved but the influence of NI/AI water is still important. On the isopycnal $\gamma_0 = 27.9$ km m^{-3} the FSC site has low potential temperature, the IFR site high and the FBC site an intermediate value. As the current–temperature sections show on this isopyc-

nal and those adjacent to it water is making its way from the FSC to IFR via FBC; thus the observed changes must result from nonconservative processes such as diapycnal mixing.

Further evidence for the action of mixing is also found in the distribution of isopycnal separation (Fig. 14b), which approximates the distribution of potential vorticity (PV). Recall that in the absence of mixing by Ertel's theorem PV $= (2\Omega + \zeta)\cdot\nabla\rho$ is conserved following the fluid. If the relative vorticity ζ remains small compared with the planetary vorticity f, as our measurements and those of Borenäs and Lundberg (1988) show, then $\nabla\rho \sim \Delta\gamma_0/h$ remains invariant. Thus h, the separation between fixed isopycnals differing in magnitude by $\Delta\gamma_0$, should remain constant. Evidently even in the passage of fluid from the channel to the ridge, a distance of only 75 km this is not so; the stratification on the ridge is highly compressed (Fig. 10) confirming the strength of mixing.

Diapycnal mixing is usually supposed to weaken stratification, smoothing out regions of large vertical gradients. However, near boundaries there are numerous observations confirming the opposite behavior; at the bottom of the surface mixed layer or at the top of the benthic mixed layer (an increase in) turbulent activity leads to sharpening of gradients. Borenäs and Lundberg (1988) estimated the Richardson number from a small number of current profiles and simultaneous CTD lowerings in the Faroe Bank Channel and found values less than unity associated with regions of strong shear. They concluded that the stratification was barely able to suppress the turbulence-generating tendency of the velocity shear. Thus, there is evidence to suggest that Kelvin–Helmholtz instability or billow turbulence is a potential agent for the diapycnal mixing inferred from the downstream variation of water properties.

Year-long measurements made by moored current meters, which will be discussed fully in the following section, permit us to make further estimates of Richardson number. The data is derived from a pair of current meters on mooring 438 at depths of 500 and 700 m approximately, the upper in warm MNA water and the lower in cold NS water. Using a T–S relation derived from contemporary CTD data, temperature has been converted to $\gamma_{0.6}$, the potential density estimated at 600 db (the mean depth of the pair of instruments). Statistics from the two instruments are shown in Table 1 (upper); in the lower part of the same table instrument differences are presented. Thus, the mean potential density difference is 0.638 kg m^{-3} and the minimum value corresponds to virtually unstratified flow. The square root of the total shear squared, $(\Delta U^2 + \Delta V^2)^{1/2}$, has a mean value near 60 cm s^{-1} and also has vanishingly small minimum values. Infrequent very large values of Richardson number, $g\Delta\gamma_{0.6}\Delta z/\rho(\Delta U^2 + \Delta V^2)$, thereby result so that Ri statistics are not given. The frequency histogram (Fig. 16) is preferred.

Despite the fact that currents have been determined as 1-hour averages and that the (squared) shear is evaluated from a finite difference representative over a depth of 200 m the Richardson numbers were generally very low. For 10 hours they were between 0.5 and 1.0, when both shear and density difference were near their maxima, and for one-third of the record they were less than 3. In the near future it is planned to repeat the observations employing shorter time intervals and smaller vertical separation, but the data already in our possession encourages our belief that billow turbulence is a potent mixing agent in the region under study.

A budget method which depends on the assumption of stationarity permits quantitative estimates of the turbulent heat flux and thereby of the effective diffusivity, see Fig. 17. On the FBC and IFR sections mass fluxes are well defined: denoting the former section *in* and the latter *out* and the 3°C surface connecting them *3*, then the mass balance (here for water colder than 3°C) may be written

$$F_{\text{in}} - F_{\text{out}} + F_3 = 0$$

TABLE 1. Current meter data from mooring 438. See Table 3 for further details.

	Instrument depth (m)							
	502				693			
	mean	min	max	std dev	mean	min	max	std dev
Temperature (°C)	7.24	−.61	8.37	1.14	−.60	−.82	5.69	0.21
Potential density (kg m^{-3})	.245	.134	.913	0.11	.883	.448	.924	0.03
Speed (cm s^{-1})	21.6	3.2	95.2	13.8	56.7	11.3	85.8	10.6
Differences		nom. 600 m						
Potential density (kg m^{-3})	.638	.004	.784	.111		g = 9.8 m s^{-2}		
Square root of shear^2 (cm s^{-1})	59	.4	125	48		ρ = 1030 kg m^{-3} Δz = 191 m		

* Note potential density is evaluated at 600 db and the figure 1030 is omitted ahead of the decimal point.

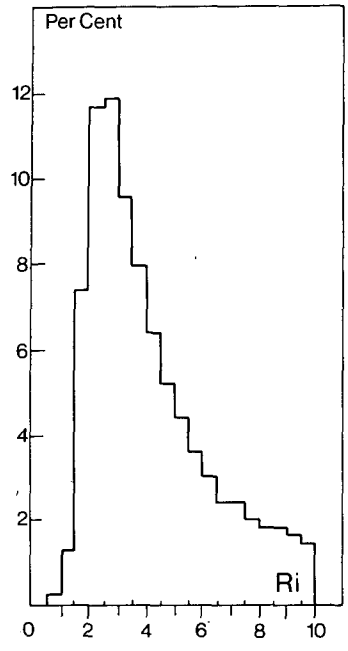

FIG. 16. Frequency histogram for Richardson numbers calculated from 8701 1-hour measurements on mooring 438: instrument separation 200 m.

($F_3 > 0$ implies entrainment from above, $F_3 < 0$ implies detrainment). The heat balance is similar but contains an additional term, the turbulent flux across the 3°C surface, namely

$$F_{in}\theta_{in} - F_{out}\theta_{out} + F_3 3 = AK\left.\frac{\partial\theta}{\partial z}\right|_3.$$

In the absence of information correlation terms are ignored. Combining these two equations leads to

$$F_{in}(3 - \theta_{in}) - F_{out}(3 - \theta_{out}) = AK\left.\frac{\partial\theta}{\partial z}\right|_3$$

where A is the area of the 3°C surface, $\partial\theta/\partial z$ is the spatially averaged gradient on that surface and K is the turbulent diffusivity. Substitution of the values given in Table 2 and derived from both the 1987 and 1988 cruises yield values of K ranging from 50–150 $cm^2\,s^{-1}$. These are surprisingly large values and serve to emphasise the role played by mixing in establishing the far field properties of the overflow. Not only do the properties of the core water such as temperature, salinity and tracers vary sharply downstream (Swift 1984) so also does potential vorticity.

3. Moored instrument measurements

As mentioned in the Introduction the principal interest in and novelty of measurements of currents from the Faroe Bank Channel lies in their long-term character; so far IOS has recovered three long-term moorings and their locations, durations and depths of instruments are shown in Table 3.

Two of the moorings 435, 438 were of year-long duration (5/87 to 5/88): the third 408 was a four-month duration (3/86 to 8/86). Information concerning mooring design, data quality and processing are described in a data report (Saunders and Gould 1989) and should be consulted for these details. The data report also contains an extensive summary of the data.

Currents and temperatures derived from the long-term deployments are reported in Table 4. The mean flow direction for the eight records is 135°–315°; so currents have been resolved into northeast or cross-channel and northwest or down-channel direction. This differs insignificantly from the 130°–310° used in the CTD/ADCP sections (Figs. 4–6). Mean values and various statistics for a low-pass version of the data are tabulated and mean down-channel flows and temperatures are indicated on Fig. 2.

As is apparent from this tabulation and also from Fig. 2, five of the records are within the warm water (>7°C) and three within the cold (<0°C). The flow in the long-channel direction for these two types of water differs in one important respect; in the cold outflow the NW component is persistent and never reverses—fluctuations in its strength, measured by the standard deviation, are *much* smaller than the mean. In the warm water, flow reversals are common with the standard deviation exceeding or at least comparable to the mean NW component. It should be noted that all the long term records in the warm water are from the south side of the channel and show a mean SE component which is ascribed to a persistent anticyclonic circulation around the Faroe Bank. Note that a persistent NW flow probably exists on the north side of the channel, the three CTD/ADCP sections reported here (Figs. 4–6) as well as those of Borenäs and Lundberg all reveal it; however, no long term current records exist from this region.

a. *Variability: days to weeks*

Spectral analysis has been performed on the low pass data from all the long-term moorings of Table 4 and representative figures from the warm water and cold water are shown (Fig. 18) in variance preserving form. Their striking characteristic is the overall predominance

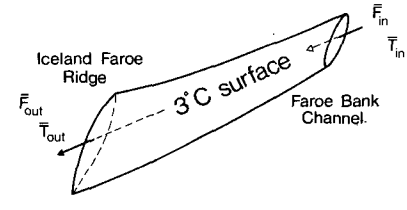

FIG. 17. The volume for which a heat budget is constructed: it is bounded above by the 3°C isotherm and below by the sea-bed.

TABLE 2. Heat budget for determination of isopycnal diffusivity.

Data source	Flux F_{in} (10^6 m^3 s^{-1})	Temperature T_{in} (°C)	Flux F_{out} (10^6 m^3 s^{-1})	Temperature T_{out} (°C)	K (cm^2 s^{-1})
Stns 2–11, 61–67					
1987	2.15	0.0	1.0	0.5	120
Stns 48–56, 61–67					
1987	2.4	0.8	1.0	0.5	80
Stns 11734–47					
1988	1.1	0.3	1.3	1.9	50

$A = 75$ km $\times$ 30 km $= 2.25 \times 10^9$ m^2.

$\left.\frac{\partial\theta}{\partial z}\right|_3 = 0.15 \pm .03$°C m^{-1} from 10 stations in discharge region.

of the down-channel over the cross-channel flow at all frequencies less than 1 cpd: the ratio of total variance derived from (Table 4) in the two components is between 10 and 20 to 1. In addition, all down-channel components have red spectra; those in the cold water have no *significant* peaks but those in the warm water have broad peaks with periods between 3 and 6 days. This band contains between 20 and 40% of the low-pass variance.

In Table 5 the coherence in this same band is presented for the currents obtained on moorings 435 and 438 (which are separated by only 3.7 km). For the down-channel component the warm water flow is strongly coherent and the flow on mooring 438 leads that on mooring 435. The coherence between warm and cold downstream components is in the noise of measurement and cannot be distinguished from zero. In the warm water the cross-channel flow is highly coherent and in phase, but between the warm and cold water components the cross-channel flow is exactly out of phase. This last result has led us compute the coherence on mooring 438 between the cross-channel flow and the depth of the thermocline drived from a thermistor chain (43804). We found that the cold water component has a coherence of 0.60 ± 0.10 and is out of phase with the depth of the 0°C isotherm. Thus, a NE flow at 700 m is associated with a thinning of the cold water layer and a SW flow associated with its thickening; no such correlation exists for the down-channel (NW) component.

TABLE 3. Mooring details.

Identification	Latitude (°N)	Longitude (°W)	Water depth (m)	Instrument depths (m)
408	61 26.7	8.13.3	746	714, 724
435	61 18.9	8.15.3	520	320, 510
438	61 20.2	8 12.3	703	302, 402, 502, TC*, 693

* Thermistor Chain 493–692 m: all other eight instruments Aanderaa RCM5.

The above observations of the cross-component of velocity and of the stratification suggest a seiche mechanism of the layers of warm and cold water; but given the phase speed of a long interfacial wave (circa 1 m s^{-1}) and the width of the channel (20 km), the period of a standing wave would be ½ day, not the 3 to 5 days observed. Kelvin waves owe their origin to the presence of a steeply sloping boundary such as exist in the channel and have zero cross channel flow; recall that in the observations the cross-channel flow is small compared with the down-channel component. However, in a two-layer flow baroclinic Kelvin waves have an amplitude inversely proportional to the layer depth (LeBlond and Mysak 1978) and so would be expected 3 to 4 times larger in the cold layer than the warm. This is quite at odds with the observations. Barotropic Kelvin waves would have equal amplitude, which is also at odds with the data. Bottom-trapped waves (Rhines 1969) have maximum amplitude at the seabed, viz. in the cold layer, and so can be discounted as an explanation of the energy in this band. In studying the Norwegian Sea overflow through the Denmark Strait, Smith (1976) identified baroclinically unstable waves (of period 2 days) by observing quadrature between the down-channel and cross-channel components and a heat flux consistent with the conversion of available potential energy from the mean to the wave (perturbation) fields. Neither of these characteristics are found in the 3–6 day period waves observed in the Faroe Bank Channel, and thus the origin and nature of these motions remains unknown.

b. Seasonal variability

A seasonal variation has been sought by fitting a sine function of annual period to monthly mean values derived from the low-pass data series and establishing the percentage of variance explained by this procedure. To test the scheme it was applied to the temperature data. All of the five warm water records showed an annual

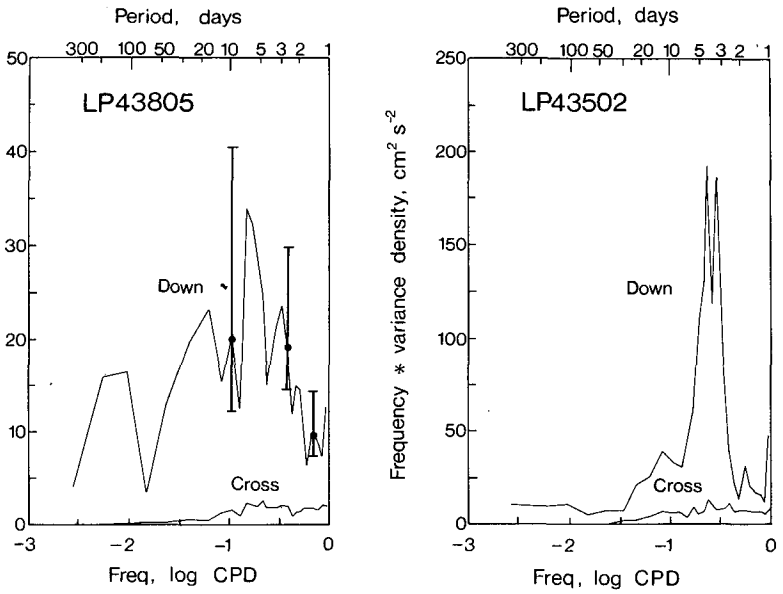

FIG. 18. Spectral variance plots in energy preserving form for cold water (left) and warm water (right). Peaks on left are probably not significant (90% confidence levels are indicated), but on right they are.

variation significant at the 90% confidence level; the amplitude of the variation was approximately 0.25°C and accounted for between 40% and 60% of the variance of the monthly mean values. Inspection of the data reveals that minimum temperatures occur in March or April and maximum in December. The lateness of the maximum is in part due to the depths concerned, 300–500 m, but no phase change can be detected. In contrast neither the cold water record from 700 m on mooring 438 shows any annual variation nor does the depth of the 3°C isotherm, derived from the thermistor chain on the same mooring. Thus, it may be asserted that there is no seasonal variation in either the thickness of the cold water outflow nor of its mean temperature (at the location of mooring 438) on the southern side of the Faroe Bank Channel.

The seasonal signal in the down-channel current components is elusive and an annual variation is found significant only in the warm water on mooring 435 which lies on the northern flank of Faroe Bank (Fig. 2). There the flow to the SE reaches a maximum in February or March and a minimum in September, the flow in late winter exceeding that in late summer by a factor of 2. Both in phase and amplitude its behaviour parallels that of the warm water inflow to the Norwegian Sea along the West Shetland Shelf edge (Gould et al. 1985). None of the records on mooring 438 reveal a seasonal variation: if it exists, its amplitude is masked

TABLE 4. Low pass data, currents and temperatures.

Ident	Depth (m)	NE (cm s^{-1}) mean	NE (cm s^{-1}) std dev	NW (cm s^{-1}) mean	NW (cm s^{-1}) std dev	Temp (°C) mean	Temp (°C) std dev	Correlation NE–NW	Correlation NW–T	Duration (days)
40801	714	−18.8	5.4	66.5	13.0	−0.22	0.24	−0.80	—	50*
40802	724	−21.3	6.4	69.3	10.0	−0.24	0.26	−0.81	—	139
43501	320	−0.4	5.1	−12.8	14.3	8.07	0.25	—	0.47	308*
43502	510	5.6	5.0	−14.4	14.2	7.50	0.46	−0.32	—	361
43801	302	0.5	6.7	−8.0	16.3	8.05	0.31	—	0.25	363
43802	402	0.6	5.6	−4.1	15.8	7.86	0.34	—	—	223*
43803	492	1.4	5.5	3.2	21.6	7.24	1.08	0.21	−0.45	363
43805	693	−3.7	2.5	56.4	9.7	−0.60	0.13	—	—	363
43804		Isotherms		5	4	3		2	1	0
		mean depth (m)		569	586	594		602	611	626
		std dev		35	35	36		35	35	32

* Short records, but data reliable. Only significant correlations reported.

TABLE 5. Coherence and phase of current fluctuations with periods 3–6 days.

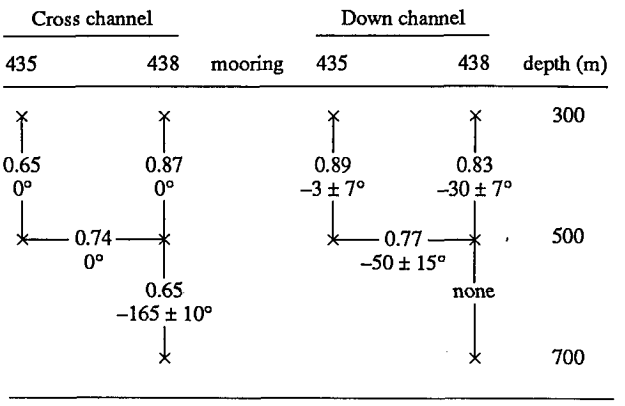

by aperiodic variation. The seasonal amplitude of the cold outflow at 700 m is determined as only 2 cm s^{-1} but an F-test shows this *not* significant at the 90% confidence level. The 4½ month long cold water records from mooring 408 do not allow a seasonal variation to be found.

c. *The cold water flux*

Although the design of the mooring array in the Faroe Bank Channel for 1987–88 called for up to six moorings in the cold outflow in order to measure its flux, of the two moorings recovered only one was in the outflow. This mooring reveals no seasonal variation in either of the attributes of the cold outflow, neither of its intensity nor of its thickness. Because the observation is made at the southern edge of the deep channel, the existence of a substantial seasonal variation in the flux of cold water, though it cannot be excluded, does seem unlikely.

By combining the yearlong results from mooring 438 (1987) with the previous year result from mooring 408 (1986) the mean outflow of water colder than say 0°C is taken to be 0.6 m s^{-1}. In order to estimate the average outflow speed for water colder than 3°C this is multiplied by 0.85 ± 0.05, a factor derived from the three sections conducted in 1987 and 1988 (Fig. 4 to 6). The cross sectional area of water colder than 3°C derived from these same sections is (3.7 ± 0.8) × 10^6 m^2. Hence the flux of cold water derived in this way from the CTD, ADCP and moored current measurements is (1.9 ± 0.4) × 10^6 m^3 s^{-1} or (1.9 ± 0.4) × 10^9 kg s^{-1}. The uncertainty, it will be noted, derives principally from ignorance about the cross sectional area occupied by the flow.

The value for the flux of cold water corresponds with the average of the three sections worked, namely 1.9 × 10^6 m^3 s^{-1} and is indistinguishable from the estimate of Borenäs and Lundberg (1988) of (1.5 ± 0.5) × 10^6 m^3 s^{-1}. On the three sections reported here the overall weighted mean temperature of the cold outflow is, from Table 2, 0.4°C corresponding to a composition of approximately 90% NS water. McCartney and Talley (1984) carried out a heat balance for the subpolar North Atlantic and Norwegian Sea and inferred a climatological cold overflow of 1.7 × 10^6 m^3 s^{-1} (T = 0°C). Since to the flow through the Faroe Bank Channel must be added the spillage over the Iceland–Faroe Ridge, reckoned to equal the outflow from the channel (Meincke 1983) plus the outflow through the Denmark Strait which though very uncertain is reckoned larger (Ross 1984) it seems probable that the estimate 1.7 × 10^6 m^3 s^{-1} will need to be revised. If further measurements confirm these assertions the estimate of the heat loss of the Norwegian Sea to the atmosphere, derived from Bunker's calculations, will need to be increased by a substantial factor.

d. *Future measurements*

The failure of the flux measurement programme as envisaged has led us to plan to revisit the Faroe Bank Channel in the autumn of 1989. A similar array of moored measurements is proposed, but in order to protect them from commercial fishing activity a short off-season deployment will be made. If coherence of the cold water outflow can be established across the width of the channel, then the case for only a small seasonal variation is established. With a comprehensive dataset, albeit of short duration, it is hoped to better establish the mean properties of the outflow, including such details as the distribution of (potential) vorticity and Froude number in order to better test models of the flow and the hypothesis of "hydraulic control." Richardson number estimates will be made on smaller time and space scales than reported here and attempts made to establish the frequency (if present) and impact of mixing events. Finally with a colleague, Dr. W. J. Gould, tests will be made of a form of acoustic tomography designed to measure the cold water flux.

Acknowledgments. The author is grateful to the numerous scientists, ships' officers and crew without whom this work could not have been carried out but particularly to Dr W. J. Gould for his help in planning and mobilizing the necessary effort and encouraging the analysis. The work at sea on RRS *Challenger* Cruise 15/87 was partially funded by UK MoD (N) as part of a Joint Research Council/Ministry of Defence Research Grants agreement.

APPENDIX

Calibration of the ADCP

On *Challenger* Cruise 15/87 attempts were made to check the performance of the Acoustic Doppler Current Profiler (ADCP). Two tests were made, one evaluating the performance in the bottom tracking mode and the other the water tracking mode.

RRS *Challenger,* like all NERC ships, has the onboard ability to compute its position at 2 minute intervals throughout a cruise. Transit satellite navigation is employed with em log data (gathered from a 1.5 m long probe) to produce the position data; a satellite fix is rejected if it is closer than about 40 minutes to the preceeding fix or if the current derived from it and the preceeding one (together with the ship's em log data) differs "unreasonably" from previous and subsequent current estimates. An element of judgement is employed.

Data was extracted from the ADCP files for the bottom navigation throughout the cruise and 1-hour averages derived; only averages were constructed if 90% of the data existed in any one hour. 104 hours of complete ADCP data was calculated and compared with the ship's motion derived from hourly positions. The results have been split into three groups according to the average ship's speed over the ground and the difference between the speed and course made good noted (see Table A1).

When underway at normal cruising speed (mean 4.75 m s^{-1}) the navigation speed and the ADCP bottom speed cannot be distinguished from each other. This is a quite remarkable result though Pollard and Read (1989) found for a similar installation on RRS *Darwin* (similar) small differences of only 1.7 cm s^{-1}. The misalignment angle for the ADCP is also gratifyingly small, 0.4° aligned to the left of the ship's direction. Note that the misalignment error has two components, the physical orientation of the sensors on the ship's hull *and* the ship's gyro compass misalignment: presumably the former is constant but, as Pollard and Read have shown, short and long term drifts in the gyro do degrade ADCP measurements. Although the underway data was split into two equal sections and the results calculated for each, the misalignment angle was not found to differ significantly amongst the two datasets. Subsequent experience suggests we were extremely fortunate in this regard.

At low speeds, 0–2 m s^{-1}, when the ship was on station (or maneuvering towards a station) differences between the ADCP and ship's navigation are larger and more uncertain, both in speed and direction. The speed correction may reflect a bias in the ADCP to read low at low speeds. (Leakage of the high energy transmitted frequency into the weak received signal may bias the measured frequency *shift* to low values). At intermediate speeds the error is intermediate. Note that all the misalignment angles have the same sign and can not be distinguished from each other.

TABLE A1. A comparison between bottom track ADCP and "hourly" satfixes.

Range of speed (m s^{-1})	Mean speed (m s^{-1})	Number of observations	Difference between satfix and ADCP	
			Speed (cm s^{-1})	Direction (°T)
0 to 2	0.8	27	6.0 ± 3.2	−1.0 ± 2.5
2 to 4	3.1	26	2.4 ± 5.0	−1.2 ± 0.8
>4	4.75	51	−0.1 ± 1.8	−0.4 ± 0.25

Attempts to check the performance of the water tracking mode were restricted to a period of the cruise when the ship was steaming at approximately 4 m s^{-1} towing the SeaSoar vehicle and CTD in a zig-zag pattern. (See Fig. 1 of Gould et al. 1987). From this 5-day portion of the cruise the 3 minute values at 10 m depth were extracted from the ADCP data. On each of the ten legs the mean ship motion over the ground was derived from ship navigation and the mean ship's motion relative to the water determined. By vector addition the current at 10 m was derived and resolved into components parallel and normal to the ship's track. Finally the ship track averages were computed weighting each values by the track duration. For 122 hours of data at a mean speed of 362 cm s^{-1} the mean current component *following* the track of the ship was 5.2 ± 1.9 cm s^{-1} and the mean current component normal to the track was 2.3 ± 1.3 cm s^{-1} from *right* to *left.*

If repeated crossings were made of the same body of water in randomly distributed directions evidently zero would be expected for both these quantities. Here we shall tentatively make this same assumption and interpret the results. In the fore and aft direction the ADCP water track reads low and speeds must be augmented by approximately 1.5%; this result is quite comparable to that of Pollard and Read. In the athwartship's direction if the observed current is interpreted as due to misalignment of ADCP sensors and gyro the angle deduced is −0.37 ± 0.16° identical to that found for the underway estimates in the bottom track mode. Similar equality of 'misalignment' in bottom tracking and water tracking modes were reported by Pollard and Read.

While combining ADCP currents and geostrophic currents only ADCP data gathered when steaming between stations was employed. Since the current component required is athwartship the fore and aft correction to the speed is irrelevant. The athwartship correction which corresponds to a left to right *correction* of 2 cm s^{-1} at 3 m s^{-1} and 3.5 cm s^{-1} at 5 m s^{-1} was applied. It is doubtful, in view of the performance of the gyro even 20 minutes after a turn (see Pollard and Read) if this correction was useful.

REFERENCES

van Aken, H. M., 1988: Transports of water masses through the Faroese Channels determined by an inverse method. *Deep-Sea Res.*, **35,** 595–617.

Borenäs, K. M., and P. A. Lundberg, 1988: On the deep water flow through the Faroe Bank Channel. *J. Geophys. Res.*, **93,** 1281–1292.

Dooley, H. D., and J. Meincke, 1981: Circulation and water masses

in the Faroese Channels during Overflow '73. *Dtsche. Hydrogr. Z.*, **34,** 41–54.

Ellett, D. J., and A. Edwards, 1978: A volume transport estimate for Norwegian Sea overflow across the Wyville-Thomson Ridge. ICES, Hydrography Committee, C.M. 1978/C: 19, 11 pp.

Flather, R. A., 1986: Results from a tidal model of the North Atlantic Ocean. *Proceedings of the Tenth International Symposium on Earth Tides,* Madrid, Consejo Superior de Investigaciones Cientificas, 970 pp.

Gould, W. J., J. Loynes and J. Backhaus, 1985: Seasonality in slope current transports N.W. of Shetland. ICES, Hydrography Committee C.M. 1985/C: 7, 13 pp.

——, J. F. Read and J. Smithers, 1987: SeaSoar profiles in the Iceland–Scotland area, May 1987. Inst. Ocean. Sci., Deacon Laboratory, Report No. 253, 50 pp.

Hansen, B., S. A. Malmberg, O. H. Saelen and S. Sterhus, 1986: Measurement of flow north of the Faroe Islands June 1986. ICES, Hydrography Committee, C.M. 1986/C: 12, 14 pp.

Hermann, F., 1967: The *T-S* diagram of the water masses over the Iceland-Faroe Ridge and the Faroe Bank Channels. *Rapp. P. V. Reun. Cons. Int. Explor. Mer,* **157,** 139–149.

Kosro, P. M., 1985: Shipboard acoustic current profiling during the coastal ocean dynamics experiment. Scripps Institution of Oceanography, 85-8, 119 pp.

LeBlond, P. H., and L. A. Mysak, 1978: *Waves in the Ocean.* Elsevier Scientific Publishing Co., 602 pp.

McCartney, M. S., and L. D. Talley, 1984: Warm-to-cold water conversion in the North Atlantic Ocean. *J. Phys. Oceanogr.,* **14,** 922–935.

Meincke, J., 1983: The modern current regime across the Greenland-Scotland Ridge. *Structure & Development of the Greenland-Scotland Ridge,* Bott, Sakov, Talwani and Thiede, Eds., Plenum Publ. Co., 637–650.

Müller, T. J., J. Meincke and G. A. Becker, 1979: Overflow '73: The distribution of water masses on the Greenland-Scotland Ridge in August/September 1973. *Ber. Inst. Meereskd.,* **62,** 172 pp.

Pollard, R. T., and J. F. Read, 1989: A method for calibrating ship-mounted acoustic doppler profiles and the limitations of gyro compasses. *J. Atmos. Oceanic Technol.*

Rhines, P., 1969: Slow oscillations in an ocean of varying depth. Part 1: Abrupt topography. *J. Fluid Mech.,* **37,** 161–189.

Ross, C. K., 1984: Temperature-salinity characteristics of the overflow water in Denmark Strait during "OVERFLOW '73." *Rapp. P. V. Reun. Cons. Int. Explor. Mer,* **185,** 111–119.

Saunders, P. M., 1985: Collection, calibration and processing of CTD data at IOS. ICES Hydrography Committee, C.M. 1985/C: 5, 14 pp.

——, 1987: Flow through Discovery Gap. *J. Phys. Oceanogr.,* **17,** 631–643.

——, and W. J. Gould, 1988: CTD data from RRS Challenger Cruise 15/87 around the Faroe Islands. Inst. Oceanogr. Sci., Deacon Laboratory, Report No. 256, 79 pp.

——, and W. J. Gould, 1989: Current measurements made around the Faroe Islands in 1986 and 1987. Inst. Oceanogr. Sci., Deacon Laboratory, Report No. 261, 80 pp.

Smith, P. C., 1976: Baroclinic instability in the Denmark Strait Overflow. *J. Phys. Oceanogr.,* **6,** 355–371.

Swift, J. H., 1984: The circulation of the Denmark Strait and Iceland-Scotland overflow waters in the North Atlantic. *Deep-Sea Res.,* **31,** 1339–1355.

Worthington, L. V., 1970: The Norwegian Sea as a mediterranean basin. *Deep-Sea Res.,* **19,** 77–84.